Egyptian Journal of Medical Microbiology Volume 34 / No.4 / October 2025 277-287 Online ISSN: 2537-0979

ORIGINAL ARTICLE

Unveiling Biological Activities of Greenly Synthesized Copper oxide Nanoparticles Using Solenostemma argel (Del.) Hayne Extract

[1]Riyam S. Jasim, [2]Ghada A. El-Sherbeny, [3]Ayman Y. El-Khateeb, [4]Mustafa M. El-Zayat*

[1]Department of Botany, Faculty of Science, Mansoura University, Mansoura 35516, Egypt; Department of Biology, College of Basic Education, University of Misan, Maysan, Iraq

[2]Department of Botany, Faculty of Science, Mansoura University, Mansoura 35516, Egypt

[3]Department of Agricultural Chemistry, Faculty of Agriculture, Mansoura University, Mansoura City 35516, Egypt

[4]Unit of Genetic Engineering and Biotechnology, Faculty of Science, Mansoura University, Mansoura 35516, Egypt; Department of Biology, Faculty of Science, New Mansoura University, New Mansoura City, Egypt

Key words:
Solenostemma argel, CuO-NPs, Antioxidant, Antimicrobial, Cytotoxic activity

Corresponding Author:
Mustafa M. El-Zayat
Unit of Genetic Engineering and Biotechnology, Faculty of Science, Mansoura University, Mansoura 35516, Egypt; Department of Biology, Faculty of Science, New Mansoura University, New Mansoura City, Egypt
mustafamohsen75@mans.edu.eg

ABSTRACT

Background*: Solenostemma argel (Del.) Hayne is a medicinal plant used in the Egyptian folk medicine. It is rich with phytochemicals that could be used in the green synthesis of copper oxide nanoparticles.* ***Objectives****: This article aims to greenly synthesize copper nanoparticles (CuO-NPs) using S. argel aqueous extract, to characterize CuO-NPs and to screen their antimicrobial, cytotoxic and antioxidant activity.* ***Methodology:*** *The CuO-NPs were prepared and characterized using various analytical techniques. The antimicrobial, cytotoxic and antioxidant activities were tested using well diffusion, MTT and DPPH assays, respectively.* ***Results and discussion:*** *The results confirmed the successful green synthesis of copper nanoparticles (CuO-NPs) using S. argel extract that was source of reducing phytochemicals like phenolics and flavonoids that were consumed in the synthesis process. The characterization techniques for CuO-NPs confirmed their size, morphology, crystallinity and stability. The antioxidant activity analysis showed IC50 values of 0.011 mg/mL for S. argel and of 0.478 mg/mL for the prepared nanocomposites that were valuable antioxidants. The prepared CuO-NPs expressed broad antimicrobial spectrum against the pathogenic bacterial strains Staphylococcus aureus, Staphylococcus epidermis, Bacillus cereus, Escherichia coli, Salmonella typhimurium and Klebsiella pneumonia and the pathogenic fungus Candida albicans. CuO-NPs showed potent anticancer potential against MDA-MB-231 breast cancer and SKOVE cells using MTT assay. The CuO-NPs have a significant cytotoxic effect (IC50) of 1184 µg/mL against MDA cells and IC50 of 911.1 µg/mL against SKOV cells.* ***Conclusion:*** *The prepared CuO-NPs could be used as a valuable alternative for antibiotics in addition to their potency as antioxidant and anticancer drugs.*

INTRODUCTION

Solenostemma argel (Del.) Hayne (family Apocynaceae) is a wild perennial plant native to North Africa and the Arabian Peninsula. It can thrive arid and semiarid habitats. It has erected stems. The leaves are simple, entire, and often oval-shaped, with a smooth texture. The flowers are small, starshaped and bloom in clusters. It produces pod like fruits[1,2].

S. argel extracts have been potentially used for synthesizing nanoparticles such as silver, gold and selenium nanocomposites. Such nanocomposites have shown promising results as anticancer, antidiabetic, wound healing, and neurodegenerative disorders treatments[3]. It has been reported that *S. argel* extracts from leaves, bark, and stems exhibited antimicrobial potential against various pathogenic bacterial strains like *Staphylococcus aureus* [4].These extracts also exhibited antioxidant activity attributed to the presence of phenolics and flavonoids. Such these extracts have shown potential free radical scavenging activity and capable of protecting cells from oxidative stress during invitro studies[5]. *S. argel* is rich in various phytochemical constituents that contribute to its medicinal properties including triterpenoids, tannins, steroids, alkaloids, saponins, monoterpenes, phytosterols[6].

S. argel has variably used in folklore medicine. It is traditionally used in remote areas for treatment of kidney and liver disease, allergies, neuralgia, sciatica, pain relief, wound healing, dysentery, loss of appetite, asthma, bronchitis, coughs, reduction of inflammation and rheumatic pain[7].

The previous studies illustrated that *S. argel* possess a promising anticancer activity attributed to the presence of compounds like 14,15-secopregnane glycosides and 15-ketopregnane glycosides, which contribute to their antiproliferative and apoptotic effects on different cell lines such as the colon cancer cell line (HCT-1161)[8].

This study aimed to environmentally synthesize CuO-NPs using the water extract of *S. argel*, and to evaluate their biological properties as antioxidant, anticancer, and antimicrobial potential.

METHODOLOGY

Plant Material:

The leaves of *S. argel* were collected from Saint Catherine Protectorate, South Sinai, Egypt and taxonomically authenticated according to Boulos[9]. 10 grams of *S. argel* leaves were extracted using 100 ml distilled water upon shaking for 30 minutes at 70°C, filtered and kept for analysis at 4 °C[10].

Phytochemical Analysis:

The total phenolics were quantified using Folin-Ciocalteu assay developed by Wolfe et al.[11] with the use of gallic acid as a standard. The total flavonoids were quantified using aluminum chloride assay developed by Zhishen et al.[12] with the use of catechin as a standard. The total tannins were assessed using vanillin-hydrochloride assay[13], with the use of tannic acid as standard.

Preparation of CuO-NPs:

0.1 M copper sulphate was prepared and dropped wisely to an equal volume of the prepared aqueous plant extract under magnetic stirring for 2 h. The mixture was subjected to UV irradiation (λ= 254 nm) for 20 min[14,15].

Structural Characterization of CuO-NPs:

Characterization of the prepared nanocomposites was done using TEM, SEM, UV-visible spectroscopy, FTIR spectroscopy, DLS, EDX and XRD Analysis.

Potential Biological Applications

Antimicrobial activity:

The antimicrobial potential of *S. argel* extract and the prepared CuO-NPs composite were screened using the agar well diffusion assay[16] against six pathogenic bacterial strains that are *Salmonella typhimurium* (ATCC®14028™), *Staphylococcus epidermidis* (ATCC®12228™), *Staphylococcus aureus* (ATCC®6538™), *Klebsiella pneumonia* (ATCC®10031™), *Bacillus cereus* (ATCC®11778™) and *Escherichia coli* (ATCC®10536™) obtained from the Unit of Genetic Engineering and Biotechnology, Faculty of Science, Mansoura University. Gentamycin was used as standard antibiotic.

Antioxidant activity:

The antioxidant activity was estimated following the DPPH• method prescribed by Kitts et al.[17]. Ascorbic acid was used as a reference standard. The IC50 values were calculated as the concentration at which 50% of DPPH scavenged. IC50 values are inversely proportional to the antioxidant activity[18].

Cytotoxic activity:

MDA-MB-231 breast cancer and SKOVE cells were seeded in a 96-well plate each has 5 × 10^3 cells, 100 µL of complete media and incubated for 24 hours at 37ºC in a 5% CO_2 atmosphere for cell adherence. Discarded the media, and 200 µL of fresh media was added to the wells designated as control. A serial dilution of CuO-*S. argel* nanocomposite was then applied for all duplicates, starting with 2,000 µg/mL. After 48 hours of incubation, discard the old media, and add 100 µL of prepared MTT (3-(4,5-Dimethyl-2-thiazolyl)-2,5-diphenyltetrazolium bromide; Acros Organics, China, Cat. No. A0413402) to each well. The plate was incubated for an additional 4 hours to allow for crystal formation. Following this, 100 µL of sodium dodecyl sulfate (SDS) was added, and the plates were left overnight at 37ºC at the exclusion of light to ensure complete dissolution of the crystals and release of color. The inhibition rate of MDA-MB-231 and SKOV cell proliferation was calculated using the following equation[19]:

Cell Proliferation Inhibition (%)={Control (OD)−$Sample\ (OD)$ /Control (OD)}∗ 100

The half-maximal inhibitory concentration (IC50) values for the tested nanocomposites on MDA-MB-231 cells and SKOV cells were estimated using GraphPad Prism 6 Software (GraphPad Software, CA, USA).

RESULTS

Nanocomposites Characterization:

UV-Visible Spectroscopy

The results obtained for the *S. argel* extract and CuO-NPs composites showed different features of absorption (**Fig. 1**) and indicated that each of them has different electronic transitions and revealed successful synthesis of the nanocomposites.

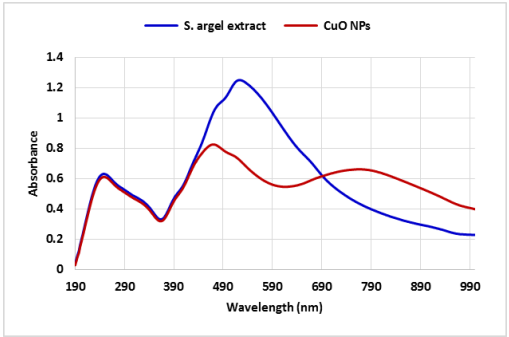

Fig. 1: UV-visible spectroscopy of *S. argel* extract and CuO-NPs.

FTIR Spectral Analysis

The FTIR analysis of *S. argel* extract and the prepared nanocomposites revealed distinct characteristic

absorption bands, indicating the presence of specific functional groups, and confirming the successful synthesis of nanoparticles (**Fig. 2**).

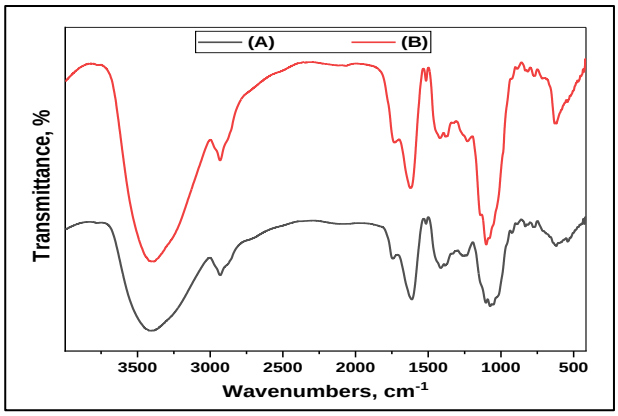

Fig. 2: FTIR spectral analysis of (a) *S. argel* extract and (b) CuO nanoparticles.

DLS Analysis

Dynamic Light Scattering (DLS) analysis was carried out to assess the size distribution and surface charge characteristics of CuO-NPs (**Fig. 3**). The DLS analysis of CuO-NPs showed a zeta average size of 887.8 nm. The polydispersity index (PDI) for these CuO-NPs nanoparticles was measured at 0.334 indicating that the particle size distribution is moderately broad. The PDI is still within an acceptable range below 0.4.

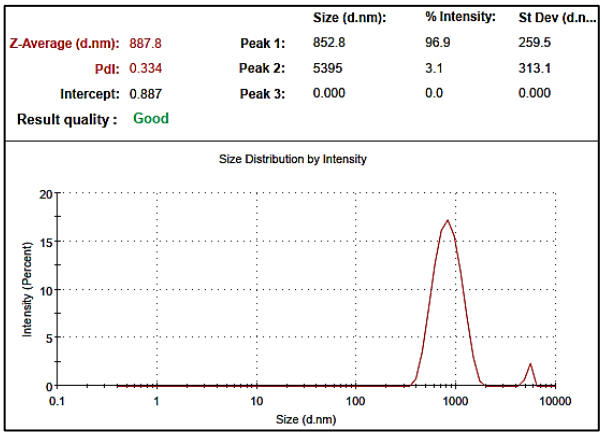

Fig 3: DLS analysis of CuO nanoparticles.

HR-TEM Analysis

CuO-NPs expressed spherical or slightly elongated shape with a good size distribution falls within the range of nanoparticles and with dark contrasts as shown in HR-TEM micrographs (**Fig 4**)

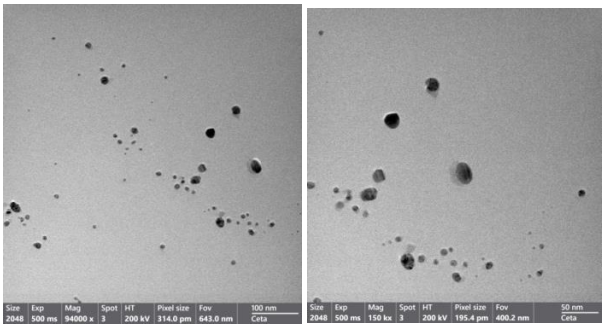

Fig. 4: HR-TEM micrographs of CuO nanoparticles.

SEM Analysis

The SEM micrographs of synthesized CuO-NPs are used to obtain a detailed morphology, structural characteristics, and agglomeration. **Figure 5** represents CuO-NPs that reveal a heterogeneous texture with irregular clusters and a highly aggregated nature, possibly due to the nature of the synthesis process involving bio reduction. The phytochemicals originating from the reducing agent tend to stabilize and cap the nanoparticles, which act to aggregate in a tightly bound manner.

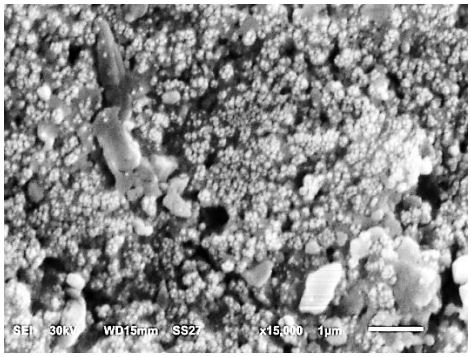

Fig. 5: SEM micrographs of CuO nanoparticles.

EDX Analysis

EDX was performed to analyse the elemental composition of CuO-NPs. It was observed that the CuO-NPs are primarily made up of atoms of O and Cu, as would be expected from the stoichiometry of CuO-NPs. Oxygen has a composition of 57.44% by weight and 77.25% by atomic percentage, proving its dominance in the nanoparticle composition, while copper contributes 29.92% by weight and 17.12% by atomic percentage. Other trace elements presented included S, Cl, K, Ca, and Zn because of residuals in the synthesis processes. Sulfur and chlorine presumably originate from metal salts used for the synthesis, and potassium and calcium may originate from environmental contamination or reagents.

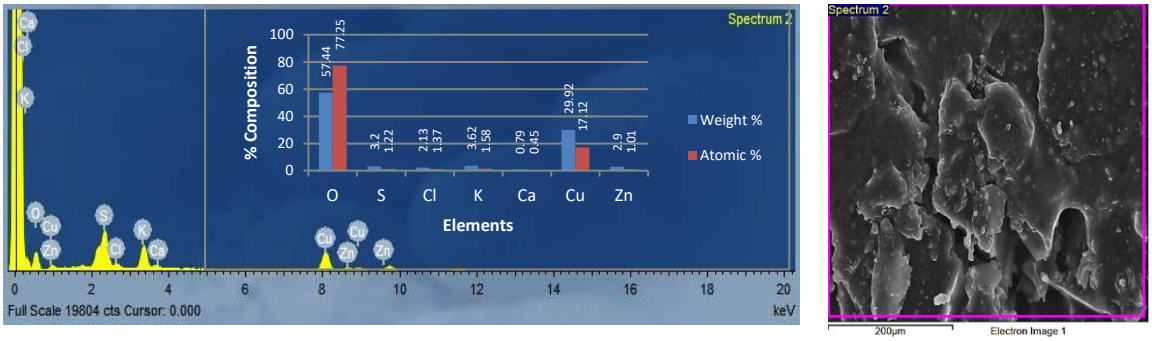

Fig. 6: EDX analysis of CuO nanoparticles.

XRD Analysis

Figure 7 presents XRD patterns of CuO-NPs, which contain key information about the structural parameters, particle size, and crystallinity of the nanoparticles. XRD analysis proves that CuO-NPs possess well-defined crystalline structures. The CuO-NPs have a monoclinic crystal structure with high crystallinity, and the sharpness of the diffraction peaks indicates this, particularly at 36.4878° corresponding to the (111) plane. The additional peaks further enhance the CuO phase and establish the purity of the material.

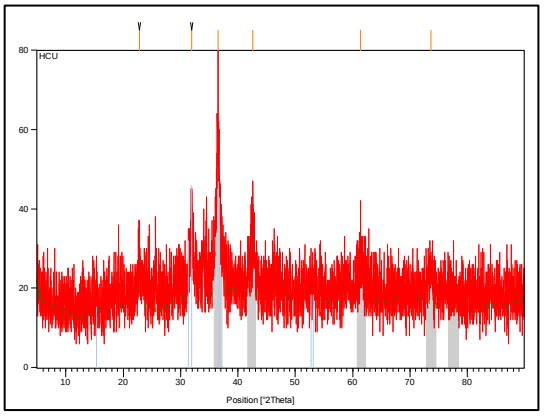

Fig. 7: XRD analysis of CuO nanoparticles.

Phytochemical Analysis

Phytochemical analysis of the investigated samples including *S. argel* extract and CuO-NPs was carried out to investigate their phenolics, flavonoids, and tannins content. The results are illustrated in **Fig 8**. *S. argel* extract exhibited the highest phenolic content with a 306.068 mg gallic acid concentration per gram of dry sample. On the other hand, CuO-NPs resulted in lower phenolic contents of 208.941 and 171.292 mg gallic acid/g, respectively. Flavonoid content followed a similar trend, as *S. argel* extract exhibited the highest value of 101.828 mg catechin/g dry sample while, CuO NPs of 22.136 mg catechin/g, that were significantly reduced.

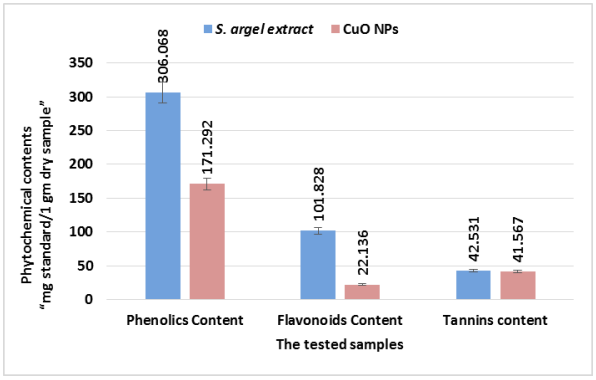

Fig. 8: A comparison of the results of the phytochemical contents of the *S. argel* extract and the prepared CuO - *S. argel* nanocomposite

Antioxidant Activity

Antioxidant activity of *S. argel* extract, the greenly synthesized nanometals, and ascorbic acid were estimated using DPPH assay and the results are represented in **Fig.** 9-10 as % remaining DPPH, % scavenging activity, and IC_{50} values The IC50 refers to the concentration at which 50% of the DPPH free radicals are scavenged, considering that IC50 values are inversely proportional to the antioxidant activity. The highest antioxidant activity was obtained for *S. argel* extract, which had IC_{50} value of 0.011 mg/mL, followed by a standard antioxidant, ascorbic acid, at an IC_{50} value of 0.022 mg/ml while that of CuO - *S. argel* nanocomposite exhibited IC_{50} value of 0.478 mg/mL.

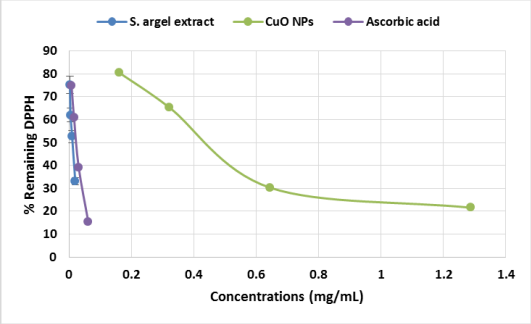

Fig. 9: The % remaining DPPH plotted versus the sample concentrations.

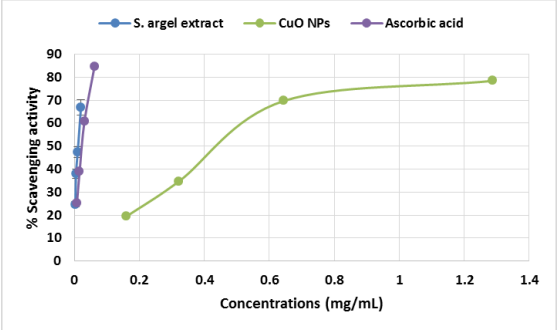

Fig. 10: The % scavenging activity plotted versus the sample concentrations.

Antimicrobial potential:

Table 1: Antimicrobial potential of the CuO nanocomposites and *S. argel* extract

Studied Bacterial species		*S. argel*-CuO nanocomposites	*S. argel*	Gentamycin
Escherichia coli	*IZ*	16	-	24
	AI	0.67	-	
Bacillus cereus	*IZ*	21	15	7
	AI	3	2.14	
Salmonella typhimurium	*IZ*	17	-	20
	AI	0.85	-	
Staphylococcus aureus	*IZ*	20	-	20
	AI	1		
Klebsiella pneumonia	*IZ*	17	-	28
	AI	0.61	-	
Staphylococcus epidermidis	*IZ*	22	-	8
	AI	2.75	-	

AI= activity index, IZ = inhibition zone (measured in mm)

The antimicrobial potential of *S. argel* extract and the prepared copper nanocomposites were evaluated and compared with the activity of the standards, viz, gentamycin. The results of antimicrobial activity are provided in Table 1 that depicts the inhibition zone (IZ) and their activity index (AI).

The results revealed that the prepared copper nano composites are potent antimicrobials that exhibited broad and efficient antimicrobial spectrum against 100% of the tested pathogens including gram positive *Staphylococcus aureus, Staphylococcus epidermis, Bacillus cereus* and gram-negative *Escherichia coli, Salmonella typhimurium* and *Klebsiella pneumonia* that was comparable with gentamycin while *S. argel* extract expressed activity against only *B. cereus* out of the tested strains.

Cytotoxic activity

The MTT assay evaluated cytotoxicity effects of CuO-NPs biosynthesized from *S. argel* extract on MDA-MB-231 breast cancer cells and Skov3 ovarian cancer cells. The cytotoxicity experiments revealed that CuO-NPs displayed dose-dependent toxicity because rising nanoparticle concentrations led to lower cell survival rates thus indicating anticancer effects. The anticancer activity of *S. argel*-derived CuO-NPs on breast cancer MDA-MB-231 cells exhibited moderate cytotoxicity with IC_{50} value of 1184 µg/mL. The cytotoxic effects of CuO-*S. argel* depended on dosage because cells remained viable at 94%, indicating it only becomes toxic at higher concentrations as illustrated in **Figure** 11. CuO-*S. argel* nanocomposite along with Skov3 ovarian cells exhibited well cytotoxic effects with IC_{50} value of 911.1 µg/mL The results revealed that as the concentration of CuO-NPs increased the suppression of cell viability increased where the highest concentration of CuO-*S. argel* (4000 µg/mL) demonstrated a 17.9% suppression of cell viability. The cytotoxicity experiments revealed that CuO-*S. argel* demonstrated increased mortality against Skov3 ovarian cancer cells and displayed lower toxicity toward MDA-MB-231 breast cancer cells thus suggesting CuO-NPs have cancer-cell type selectivity as illustrated in **Figures.**12 and 13.

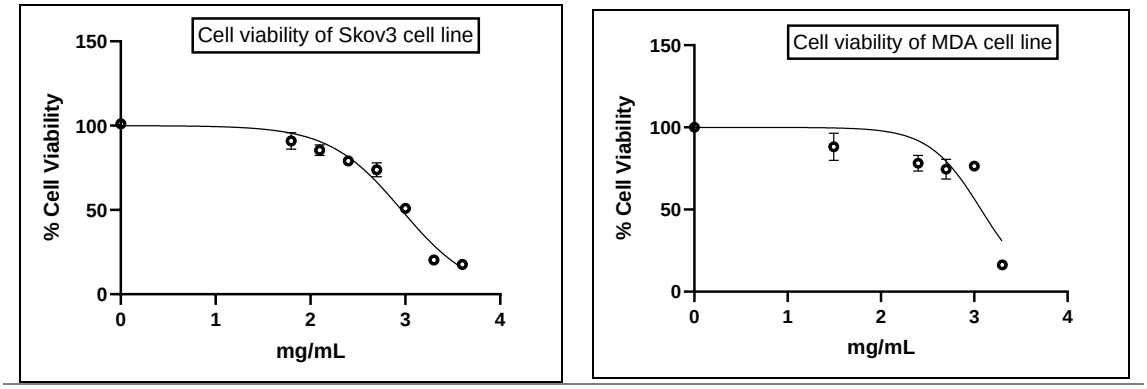

Fig 11: The cell viability of Skov3 and MDA cell lines using CuO- *S. argel* nanocomposite

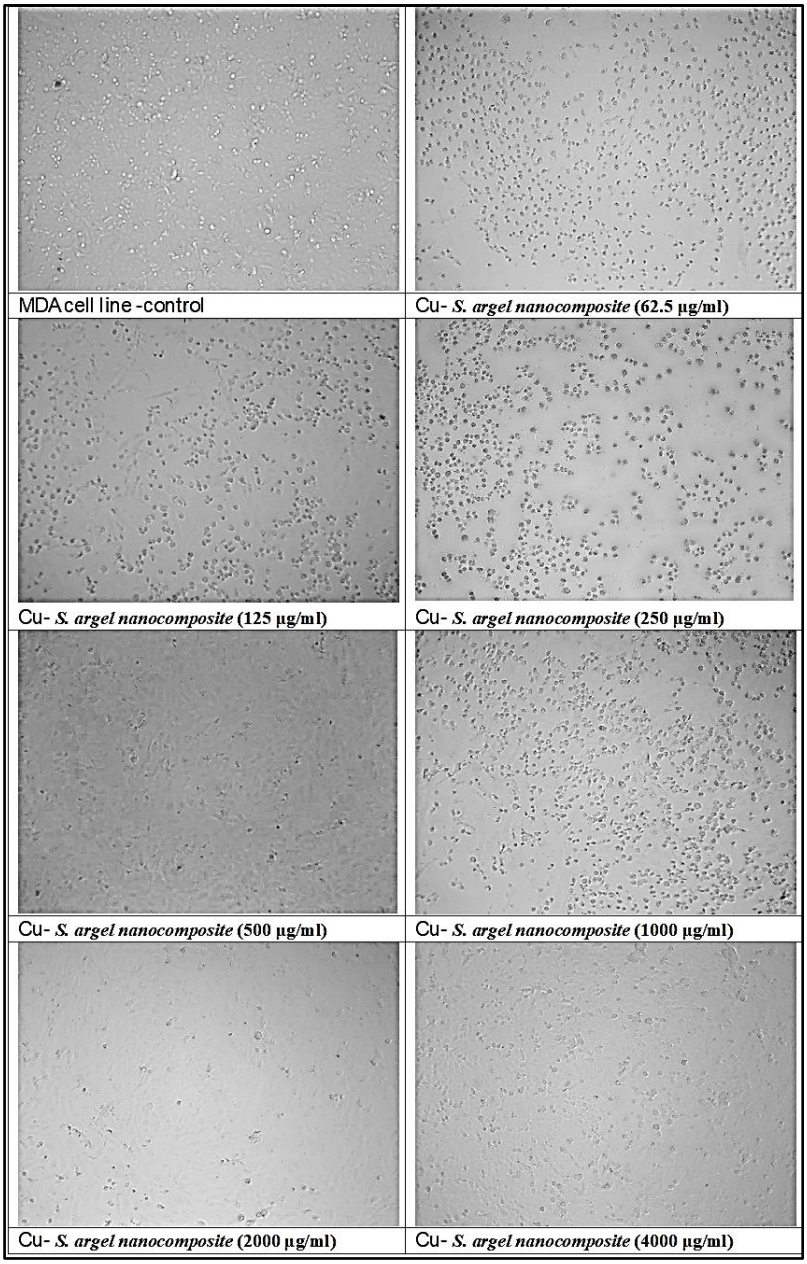

Fig. 12: MTT assay images showing the viability of treated MDA cell lines CuO NPs

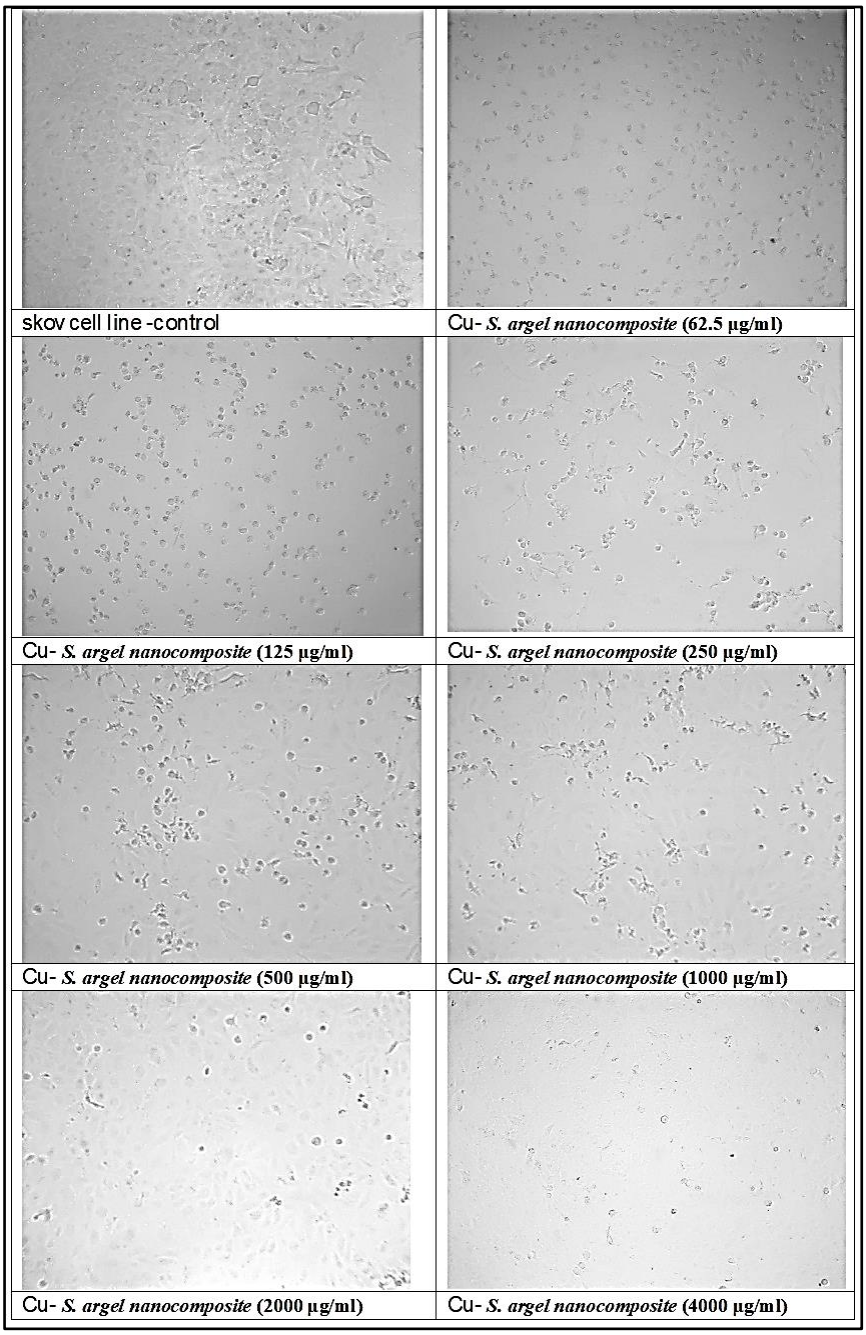

Fig 13: MTT assay images showing the viability of treated SKOV cell lines CuO NPs

DISCUSSION

The CuO-NPs were biosynthesized using *S. argel* extract and characterized using various analytical techniques.

S. argel extract showed maximum absorbance at 523.0 nm using UV-Visible spectroscopy due to $\pi \rightarrow \pi^*$ transitions of flavonoids and phenolics that would act as reducing agents in the nanoparticle synthesis process. CuO-NPs exhibited double absorptions peaks at 766.0 nm and 470.0 nm, due to d-d transitions of the electronic states in copper ions, charge transfer transitions confirmed that the copper oxide has undergone nano dimensional transformation. These results confirm the green synthesis methodology using *S. argel* extract and point to the successful preparation of CuO-NPs with well-defined optical properties[20,21].

The IR spectrum of *S. argel* extract showed a strong absorption band at 3407 cm^{-1}, which is attributed to the stretching vibration of hydroxyl groups "O-H". Aliphatic hydrocarbons appeared at 2932 cm-1 owing to the stretching vibrations of C-H groups. A strong

absorption band appeared at 1744 cm^{-1} indicated the presence of carbonyl "C=O" groups, while the absorption bands appeared at 1613 cm^{-1} suggested stretching vibrations of C=C of aromatic skeletons. The absorption bands in the 1414-1384 cm^{-1} region presented C-H or C-O bending. Consequently, absorption peaks between 1261-1237 cm^{-1} have been attributed to C-O stretching in esters or ethers. Hence, absorption bands appearing at 3385, 2933, and 1724 cm^{-1} can be assigned to O-H stretching frequency, C-H stretching frequency, and C=O stretching frequency, respectively[22,23]. Besides, in the analysis of CuO-NPs, the confirmation of the formation of Cu-O is specified by the presence of metal-oxygen vibrations of Cu-O at 631 cm^{-1} and 510-469 cm^{-1} [24]. The results of FTIR spectral analysis confirmed the participation of the functional groups in the plant extract that were responsible for the formation of metal nanoparticles, in addition to the formation of metal-oxygen groups appeared in the analysis of nanoparticles samples.

Zeta average large size of of 887.8 nm indicates that the CuO-NPs tend to aggregate or agglomerate in the aqueous dispersion, which is a common occurrence during nanoparticle synthesis, especially when biomolecules are involved in the process[25]. The *S. argel* extract likely plays a role in stabilizing the particles, though it might not completely prevent aggregation. The polydispersity index (PDI) for these CuO-NPs was measured at 0.334 indicating that the particle size distribution is moderately broad. The PDI is still within an acceptable range (below 0.4) suggesting that the CuO-NPs exhibit a reasonably controlled size distribution[26].

The dark contrasts of CuO-NPs in the HR-TEM images attributed to the high electron density of the metal oxide nanoparticles. These spherical or slightly elongated morphologies of CuO-NPs are typical for their crystal structures and infer a very well-controlled synthesis process[21].

SEM analysis indicated that CuO-NPs have a rough and porous surface area that enhances their surface reactivity. The nanoscale dimensions obtained from the SEM images make suggestions of high surface area-to-volume ratios, which is appropriate for functional applications. However, aggregation may reduce the number of active sites available on their surface, hence decreasing their efficiency[27].

EDX analysis approved the elemental composition of CuO-NPs. Also, General results from the XRD measurement indicate that nanoparticles of CuO have been produced with high crystallinity and these can be highly promising candidates in advanced applications.

The phytochemical results showed a decrease in the phenolics, and flavonoids content in CuO nanocomposite than *S. argel* extract that might be attributed to their utilization in the reduction of the metals ions during the synthesis of the nanoparticles where these compounds might be degraded or transformed during the synthesis of nanoparticles. On the Contrary, tannins content did not reveal distinct variation because tannins might be more stable than other polyphenolic groups in the process of synthesizing nanoparticles[28,29]. The results of phytochemical analysis showed that the extract of *S. argel* is rich in phenolics, flavonoids, and tannins and hence a potential candidate for the synthesis of nanoparticles. The reduction in the content of phytochemical contents reveals the impact of the synthesis process on the stability and retention of bioactive compounds. Higher retention of tannins than flavonoids and phenolics in nanoparticles would have suggested a potential role of tannin in the stabilization of the nanoparticle structure[30].

The results showed that *S. argel* extract has a very potent antioxidant capability considering that IC50 values are inversely proportional to the antioxidant activity[31], most probably due to its high content of phenolics and flavonoids, as was already obtained from the phytochemical study. On the other hand, the CuO-*S. argel* nanocomposite exhibited moderate antioxidant activity through this study, likely due to a reduced retention of bioactive compounds or the consumption of phenolics and flavonoids during the nanoparticle biosynthesis process[30].

It was previously reported that, the antimicrobial activity of copper oxide nanoparticles has garnered significant attention regarding their antimicrobial potential as alternatives to traditional antibiotics against antibiotic resistant pathogenic microorganisms. CuO nanocomposite follow different mechanisms of action against bacterial strains. The small size and high surface-to-volume ratio of the nanoparticles promote proper interaction with microbial membranes, facilitating effective disruption of microbial membranes[32]. This could occur through electrostatic Interaction as the negative charge of bacterial cell surfaces allows for adhesion of positively charged copper ions from the nanoparticles, leading to cell membrane disruption and consequent cell death, generation of Reactive Oxygen Species (ROS) where Copper ions can catalyse reactions that produce ROS, leading to oxidative stress, which damages DNA, proteins, and lipids within the bacterial cells and formation of Cavities and Cell Lysis that cause morphological changes in bacteria, leading to cell lysis and disruption of the integrity of the cell wall[33,34].

The MTT assay results indicated that the control of cancer cell killing effects of CuO-NPs synthesized from *S. argel* depends on nanoparticle elements, dosage amount as well as specific cancer cell types. Both cancer cell lines experienced greater toxicity from CuO-NPs due to the combination of competitive factors that include smaller size and superior surface reactivity along with enhanced cellular uptake[35]. The cytotoxic activity of CuO-NPs for cancer cells depends on cell

line concentration because oxidative stress and mitochondrial targeting contribute together to their toxic properties[36]. CuO-NPs demonstrate augmented cytotoxic effects because they produce reactive oxygen species (ROS) that attack DNA proteins and lipids inside cells. Several scientific investigations have proven that copper nanoparticles cause cancer cell apoptosis through mechanisms based on reactive oxygen species generation[36,37]. The superior cytotoxicity of CuO-NPs against Skov3 cells occurs because these ovarian cancer cells are more reactive to oxidative damage together with mitochondrial dysfunction compared to MDA-MB-231 cells[38,39,40]. The cytotoxic effectiveness of CuO-NPs increases because of the bioactive phytochemicals present in *S. argel* extract used to reduce and stabilize the nanoparticles during the synthesis process. Biosynthesized CuO-NPs benefit from anticancer properties because phytochemicals enhance their activity through stabilization of nanoparticles and better cell uptake that would enhance biological activity of synthesized nanoparticles.

CONCLUSION

This study demonstrated the synergistic relationship between the extract of *S. argel* and the synthesized CuO-NPs. The findings suggest that the products developed in this research could serve as alternatives to antibiotics. Additionally, the results indicated that the synthesized CuO-NPs is promising for the treatment of breast and ovarian cancer.

REFFERENCES

1. El-Shiekh RA, Al-Mahdy DA, Mouneir, S. M, Hifnawy MS, Abdel-Sattar EA. Anti-obesity effect of *argel* (*Solenostemma argel*) on obese rats fed a high fat diet. Journal of ethnopharmacology. 2019; *238*, 111893.
2. Perrone A, Plaza A, Hamed A, Pizza C, Piacente S. *Solenostemma argel*: a rich source of very unusual pregnane and 14, 15-secopregnane glycosides with antiproliferative activity. *Current Organic Chemistry*. 2008; *12*(18), 1648-1660.
3. Abdel-Sattar E, El-Shiekh RA. A Comprehensive Review on *Solenostemma argel* (Del.) Hayne, an Egyptian Medicinal Plant. Bulletin of Faculty of Pharmacy Cairo University. 2024; 62(1), 3.
4. Hamadnalla HM, El Jack MM. Phytochemical screening and antibacterial activity of *Solenostemma argel*: A medicinal plant. *Acta Scientific Agriculture*. 2019; 3(6), 2-4.
5. Elsanhoty RM, Soliman MS, Khidr YA, Hassan GO, Hassan AR, Aladhadh M, Abdella A. Pharmacological activities and characterization of phenolic and flavonoid compounds in Solenostemma argel extract. Molecules. 2022; 27(23), 8118.
6. Abdel-Sattar E, El-Shiekh RA. A Comprehensive Review on *Solenostemma argel* (Del.) Hayne, an Egyptian Medicinal Plant. Bulletin of Faculty of Pharmacy Cairo University. 2024; 62(1), 3.
7. Abdel-Motaal FF, Maher ZM, Ibrahim SF, El-Mleeh A, Behery M, Metwally AA. Comparative studies on the antioxidant, antifungal, and wound healing activities of *Solenostemma argel* ethyl acetate and methanolic extracts. Applied Sciences. 2022; 12(9), 4121.
8. Maad AH, AL-Gamli AH, Shamarekh KS, Refat M, Shayoub ME. Antiproliferative and Apoptotic Effects of *Solenostemma argel* Leaf Extracts on Colon Cancer Cell Line HCT-116. Biomedical and Pharmacology Journal. 2024; 17(3), 1987-1996.
9. Boulos L. Flora of Egypt. 2000; 2: 1-352. Al Hadara Publishing, Cairo.
10. El-Zayat MM, Eraqi MM, Alrefai H, El-Khateeb AY, Ibrahim MA, Aljohani HM, Elshaer MM. The antimicrobial, antioxidant, and anticancer activity of greenly synthesized selenium and zinc composite nanoparticles using Ephedra aphylla extract. Biomolecules. 2021; 11(3), 470.
11. Wolfe K, Wu X, Liu R. Antioxidant activity of apple peels. Journal of Agricultural and Food Chemistry. 2003; 51: 609-614.
12. Zhishen J, Mengcheng T, Jianming W. Research on antioxidant activity of flavonoids from natural materials, Food Chemistry Journal. 1999; 64:555-559.
13. Kitts DD, Wijewickreme AN, Hu C. Antioxidant properties of a North American ginseng extract. Molecular and cellular biochemistry. 2000; 203, 1-10.
14. Dent M, Dragović-Uzelac V, Penić M, Bosiljkov T, Levaj B. The effect of extraction solvents, temperature and time on the composition and mass fraction of polyphenols in Dalmatian wild sage (*Salvia officinalis* L.) extracts. Food technology and biotechnology. 2013; 51(1), 84-91.
15. Supraja S, Ali SM, Chakravarthy N, Jaya Prakash Priya A, Sagadevan E, Kasinathan MK, Arumugam P. Green synthesis of silver nanoparticles from *Cynodon dactylon* leaf extract. Int J Chem Tech. 2013; 5(1), 271-277.
16. Khosravi AR, Khosravi A, Khosravi M. Antimicrobial activity of various plant extracts against common pathogens: A well diffusion assay approach. Journal of Medicinal Plants Research. 2020; 14(5), 123-130.

17. Kitts DD, Hu X. "Antioxidant activity of the extracts of various plant materials." *Food Chemistry*. 2003; 81(2), 223-229. doi:10.1016/S0308-8146(02)00366-0.
18. Khalil MM, Khedher NB. "Antioxidant activity and phenolic content of some Tunisian medicinal plants." Journal of Medicinal Plants Research. 2018; 12(1), 1-9. doi:10.5897/JMPR2017.6340.
19. Kumar, S, *et al.* Cytotoxicity and apoptosis induction by a novel compound in MDA-MB-231 breast cancer cells. Journal of Cancer Research and Clinical Oncology. 2018; 144(5), 927-938. doi:10.1007/s00432-018-2580-5.
20. Attar, K, *et al.* Green synthesis of metal nanoparticles using plant extracts: A review. Journal of Nanostructure in Chemistry. 2020; 10(1), 1-15. doi:10.1007/s40097-020-00345-0.
21. Neiva J, Benzarti Z, Carvalho S, Devesa S. Green Synthesis of CuO Nanoparticles-Structural, Morphological, and Dielectric Characterization. Materials (Basel, Switzerland). 2024; 17(23), 5709. https://doi.org/10.3390/ma17235709
22. Zhang M, Ding R, Hu F. Comparison on FTIR spectrum and thermal analysis for four types of *Rehamnnia glutinosa* and their extracts. 2022; https://doi.org/10.21203/rs.3.rs-1319441/v1.
23. Syafinar R, Gomesh N, Irwanto M, Fareq M, Irwan YM. FT-IR and UV-VIS spectroscopy photochemical analysis of dragon fruit. ARPN J. Eng. Appl. Sci. 2015; *10*(15), 6354-6358.
24. Ferraro JR, Ferraro JR. Metal-Oxygen Vibrations. Low-Frequency Vibrations of Inorganic and Coordination Compounds. 1971; 65-109.
25. Sousa VS, Teixeira MR. Aggregation kinetics and surface charge of CuO nanoparticles: the influence of pH, ionic strength and humic acids. Environmental Chemistry. 2013; *10*(4), 313-322.
26. Eid AM, Fouda A, Hassan SED, Hamza MF, Alharbi NK, Elkelish A, Salem WM. Plant-based copper oxide nanoparticles; biosynthesis, characterization, antibacterial activity, tanning wastewater treatment, and heavy metals sorption. Catalysts. 2023; *13*(2), 348.
27. Rath PC, Patra J, Saikia D, Mishra M, Chang JK, Kao HM. Highly enhanced electrochemical performance of ultrafine CuO nanoparticles confined in ordered mesoporous carbons as anode materials for sodium-ion batteries. Journal of Materials Chemistry A. 2016; *4*(37), 14222-14233.
28. Singh J, Dutta T, Kim KH, Rawat M, Samddar P, Kumar P. Green synthesis of metals and their oxide nanoparticles: applications for environmental remediation. Journal of nanobiotechnology. 2018; *16*, 1-24.
29. Marslin G, Siram K, Maqbool Q, Selvakesavan RK, Kruszka D, Kachlicki P, Franklin G. Secondary metabolites in the green synthesis of metallic nanoparticles. Materials. 2018; *11*(6), 940.
30. Radulescu DM, Surdu VA, Ficai A, Ficai D, Grumezescu AM, Andronescu E. Green synthesis of metal and metal oxide nanoparticles: a review of the principles and biomedical applications. International journal of molecular sciences. 2023; 24(20), 15397.
31. Idamokoro EM, Afolayan AJ. In vitro evaluation of the phytochemical and antioxidant properties of *Bulbine abyssinica* Extracts. International Journal of Agriculture and Biology. 2020; *24*(6), 1781-1787.
32. Godoy-Gallardo M, Eckhard U, Delgado LM, de Roo Puente YJ, Hoyos-Nogués M, Gil FJ, Perez RA. Antibacterial approaches in tissue engineering using metal ions and nanoparticles: From mechanisms to applications. Bioactive Materials. 2021; *6*(12), 4470-4490.
33. Godoy-Gallardo M, Eckhard U, Delgado LM, de Roo Puente YJ, Hoyos-Nogués M, Gil FJ, Perez RA. Antibacterial approaches in tissue engineering using metal ions and nanoparticles: From mechanisms to applications. Bioactive Materials. 2021; 6(12), 4470-4490.
34. Sharma P, Goyal D, Chudasama B. Antibacterial activity of colloidal copper nanoparticles against Gram-negative (*Escherichia coli* and *Proteus vulgaris*) bacteria. Letters in Applied Microbiology. 2022; 74(5), 695-706.
35. Fröhlich E. The role of surface charge in cellular uptake and cytotoxicity of medical nanoparticles. International Journal of nanomedicine. 2012; 5577-5591.
36. Dolati M, Tafvizi F, Salehipour M, Komeili Movahed T, Jafari P. Biogenic copper oxide nanoparticles from *Bacillus coagulans* induced reactive oxygen species generation and apoptotic and anti-metastatic activities in breast cancer cells. *Scientific Reports*. 2023; 13(1), 3256.
37. Farshori NN, Siddiqui MA, Al-Oqail MM, Al-Sheddi ES, Al-Massarani SM, Ahamed M, Al-Khedhairy AA. Copper oxide nanoparticles exhibit cell death through oxidative stress responses in human airway epithelial cells: a mechanistic study. Biological Trace Element Research. 2022; *200*(12), 5042-5051.
38. Barboza JR, Pereira FAN, Vasconcelos CC, de Sousa Ribeiro MN, Lopes AJO. Molecular mechanisms of action and chemosensitization of

tumor cells in ovarian cancer by phytochemicals: A narrative review on pre-clinical and clinical studies. Phytotherapy Research. 2023; 37(6), 2484-2512.

39. Pourmadadi M, Holghoomi R, Maleki-baladi R, Rahdar A, Pandey S. Copper nanoparticles from chemical, physical, and green synthesis to medicinal application: a review. Plant Nano Biology. 2024;100070.
40. Wani AK, Akhtar N, Mir TUG, Singh R, Jha PK, Mallik SK, Prakash A. Targeting apoptotic pathway of cancer cells with phytochemicals and plant-based nanomaterials. Biomolecules. 2023; 13(2), 194.